



**HAL**  
open science

# Time Versus Energy in the Averaged Optimal Coplanar Kepler Transfer towards Circular Orbits

Bernard Bonnard, Helen Henninger, Jana Nemcova, Jean-Baptiste Pomet

## ► To cite this version:

Bernard Bonnard, Helen Henninger, Jana Nemcova, Jean-Baptiste Pomet. Time Versus Energy in the Averaged Optimal Coplanar Kepler Transfer towards Circular Orbits. 2013. hal-00918633v1

**HAL Id: hal-00918633**

**<https://inria.hal.science/hal-00918633v1>**

Preprint submitted on 17 Dec 2013 (v1), last revised 21 Aug 2015 (v6)

**HAL** is a multi-disciplinary open access archive for the deposit and dissemination of scientific research documents, whether they are published or not. The documents may come from teaching and research institutions in France or abroad, or from public or private research centers.

L'archive ouverte pluridisciplinaire **HAL**, est destinée au dépôt et à la diffusion de documents scientifiques de niveau recherche, publiés ou non, émanant des établissements d'enseignement et de recherche français ou étrangers, des laboratoires publics ou privés.

# TIME VERSUS ENERGY IN THE AVERAGED OPTIMAL COPLANAR KEPLER TRANSFER TOWARDS CIRCULAR ORBITS

B. BONNARD, H. HENNINGER, J. NĚMCOVÁ, AND J.-B. POMET

ABSTRACT. The aim of this note is to compare the averaged optimal coplanar transfer towards circular orbits when the costs are the transfer time and the energy consumption. While the energy case leads to analyze a  $2D$ -Riemannian metric using the standard tools of Riemannian geometry (curvature computations, geodesic convexity), the time minimal case is associated to a Finsler metric which is not smooth. Nevertheless a qualitative analysis of the geodesic flow is given in this article to describe the optimal transfers.

## 1. INTRODUCTION

We consider the controlled Kepler equation describing orbital transfers that we normalize as

$$\frac{d^2 q}{dt^2} = -\frac{q}{\|q\|^3} + u \quad (1)$$

in the case of low propulsion and the control is constrained by  $\|u\| \leq \varepsilon$  (small parameter). Let  $K = \frac{1}{2}(\frac{dq}{dt})^2 - 1/\|q\|$  be the mechanical energy of the system. The elliptic domain in the following  $(q, \frac{dq}{dt})$  space, foliated by ellipses of the free motion:

$$X = \{K < 0, q \wedge \frac{dq}{dt} \neq 0\},$$

On this domain, one can choose coordinates  $x$  related to first integrals of the uncontrolled motion that describe the geometry of the ellipses. Adding the longitude  $l$  defining the position of the spacecraft on its orbits, the system can be written in the coplanar case as:

$$\frac{dx}{dt} = \sum_{i=1,2} u_i F_i(x, l), \quad \frac{dl}{dt} = \Omega(x, l),$$

where the control  $u = (u_1, u_2)$  is represented in a moving frame  $F_1, F_2$ , e.g., the tangential/normal frame.

The energy minimization case was analyzed in a series of articles [5, 6], [8, 7], [2]; the extremal trajectories parametrized by Pontryagin maximum principle are given by the Hamiltonian

$$H(x, p, l) = \frac{1}{2}(H_1^2 + H_2^2)$$

where  $H_i(x, p, l) = \langle p, F_i(x, l) \rangle$  are the Hamiltonian lifts of the vector fields  $F_i$ . Using periodicity with respect to the longitude  $l$ , we may use a  $C^0$ -approximation in a time duration  $1/\varepsilon$  (and numerically almost indistinguishable of the true

---

Submitted to *Acta Mathematicae Applicandae*, December 12, 2013.

The second author was partially supported by *Thales Alenia Space* and *région Provence Alpes Côte d'Azur*.

trajectories), provided by trajectories of the averaged Hamiltonian

$$H(x, p) = \frac{1}{2\pi} \int_0^{2\pi} H(x, p, l) dl.$$

This Hamiltonian is associated to a Riemannian metric whose coefficients can be explicitly computed. In the coplanar case the geodesic flow is Liouville integrable and the orbital transfer towards circular orbits is related to a flat metric in suitable explicit coordinates and hence the minimizing solutions can be easily computed (straight lines in such coordinates) [2]. Moreover this result is still true if the thrust is oriented only in the tangential direction [3].

The same averaging technique can be applied in the minimum time case and leads roughly to analyze the Hamiltonian

$$H(x, p) = \int_0^{2\pi} \sqrt{H_1^2 + H_2^2} dl.$$

Despite the formal analogy with the energy case and as observed in the article [1] this Hamiltonian is associated to a non smooth Finsler metric and moreover the quadrature cannot be explicitly performed. Due to technical problems going from Riemannian to non smooth Finsler geometry the computations of transfer towards circular orbits is a complicated problem.

The objective of this article is to make a preliminary qualitative description of the time minimum transfers and to compare them with the minimum energy ones: section 2 recalls the equations and the computation of the average Hamiltonians; section 3 recalls the results from [2, 3] on the minimum energy problem; section 4 provides a new analysis of the minimum time problem, for transfers to circular orbits, and in particular proves that the elliptic domain is geodesically convex in this case; section 5 explains why that proof fails in the minimum energy problem, which is consistent with the non-convexity mentioned in [2].

## 2. PRELIMINARIES

**2.1. Coordinates.** First of all, we recall the equations describing the planar controlled Kepler problem in the elliptic case (negative energy).

If we chose as coordinates  $(n, e_x, e_y, l)$  where  $n$  is the mean movement ( $n = \sqrt{1/a^3} = (-2K)^{3/2}$ ),  $(e_x, e_y)$  are the coordinates of the eccentricity vector in a fixed frame and  $l$  is the “longitude”, or the polar angle with respect to a fixed direction, the elliptic domain is given by  $\{n > 0, e_x^2 + e_y^2 < 1\}$  and the control system is described by the Gauss equations, where  $u_t, u_n$  are the coordinates of the control in the tangential-normal frame:

$$\frac{dn}{dt} = -3n^{2/3} \frac{\sqrt{1 + 2(e_x \cos l + e_y \sin l) + e_x^2 + e_y^2}}{\sqrt{1 - e_x^2 - e_y^2}} u_t \quad (2a)$$

$$\begin{aligned} \frac{de_x}{dt} = n^{-1/3} & \frac{\sqrt{1 - e_x^2 - e_y^2}}{\sqrt{1 + 2(e_x \cos l + e_y \sin l) + e_x^2 + e_y^2}} \\ & \times \left[ 2(\cos l + e_x) u_t - \frac{\sin l + 2e_y + 2e_x e_y \cos l - (e_x^2 - e_y^2) \sin l}{\sqrt{1 - e_x^2 - e_y^2}} u_n \right] \end{aligned} \quad (2b)$$

$$\frac{de_y}{dt} = n^{-1/3} \frac{\sqrt{1 - e_x^2 - e_y^2}}{\sqrt{1 + 2(e_x \cos l + e_y \sin l) + e_x^2 + e_y^2}} \times \left[ 2(\cos l + e_x) u_t - \frac{\cos l + 2e_x + (e_x^2 - e_y^2) \cos l + 2e_x e_y \sin l}{\sqrt{1 - e_x^2 - e_y^2}} u_n \right] \quad (2c)$$

$$\frac{dl}{dt} = n \frac{(1 + e_x \cos l + e_y \sin l)^2}{(1 - e^2)^{3/2}}. \quad (2d)$$

It will be more convenient to use, instead of  $e_x, e_y$ , the eccentricity  $e$  and the argument of the pericenter  $\omega$ , defined by

$$e_x = e \cos \omega, \quad e_y = e \sin \omega, \quad (3)$$

singular at circular orbits  $e = 0$ , whence the denominator in (4d) below:

$$\frac{dn}{dt} = -\frac{3n^{2/3}}{\sqrt{1 - e^2}} \left[ \sqrt{1 + 2e \cos v + e^2} u_t \right] \quad (4a)$$

$$\frac{de}{dt} = \frac{\sqrt{1 - e^2}}{\sqrt[3]{n}} \frac{1}{\sqrt{1 + 2e \cos v + e^2}} \left[ 2(e + \cos v) u_t - \sin v \frac{1 - e^2}{1 + e \cos v} u_n \right] \quad (4b)$$

$$\frac{d\omega}{dt} = \frac{\sqrt{1 - e^2}}{e \sqrt[3]{n}} \frac{1}{\sqrt{1 + 2e \cos v + e^2}} \left[ (2 \sin v) u_t + \frac{2e + \cos v + e^2 \cos v}{1 + e \cos v} u_n \right] \quad (4c)$$

$$\frac{dl}{dt} = n \frac{(1 + e \cos v)^2}{(1 - e^2)^{3/2}} \quad (4d)$$

where the angle  $v$  is the true anomaly:

$$v = l - \omega. \quad (5)$$

In these coordinates, the elliptic domain is

$$X = \{x = (n, e, \omega), \quad n > 0, \quad 0 \leq e < 1, \quad \omega \in S^1\}. \quad (6)$$

*Remark 2.1* (Transfer towards a circular orbit). In the transfer ‘‘towards a circular orbit’’ (or if we do not care for the direction of the major axis), we may use these coordinates although they are singular at  $e = 0$ , because the variable  $\omega$  may be simply ignored; this is possible because it is a cyclic variable, i.e. it does not influence the evolution of the other variables  $(n, e, v)$ . In the variables  $(n, e)$ , we consider that the elliptic domain is:

$$\mathcal{X} = \{(n, e), \quad 0 < n < +\infty, \quad -1 < e < 1\}. \quad (7)$$

Allowing negative values of  $e$  comes from identifying  $(-e, \omega)$  with  $(e, \omega + \pi)$ ; thus considering that  $(e_x, e_y)$  (see (3)) lies on a line of fixed arbitrary direction instead of a half line. It may for instance be the line  $e_y = 0$ , and  $\mathcal{X}$  is then identified with  $\Sigma_0 = \{(n, e_x, e_y), \quad n > 0, \quad e \in ]-1, +1[, \quad e = e_x, \quad e_y = 0\}$ .

Equations (4) read:

$$\frac{dx}{dt} = \sum_{1 \leq i \leq 2} u_i F_i(x, l) u, \quad \frac{dl}{dt} = \Omega(x, l) \quad (8)$$

where  $u_1, u_2$  stand for  $u_n, u_t$ , and

$$\Omega(x, l) = n \frac{(1 + e \cos(l - \omega))^2}{(1 - e^2)^{3/2}}. \quad (9)$$

One way to introduce averaging is to use the so-called “mean eccentric anomaly”. The eccentric anomaly is  $E$ , related to  $e$  and  $v$  by

$$\tan \frac{v}{2} = \sqrt{\frac{1+e}{1-e}} \tan \frac{E}{2} \quad (10)$$

and the mean eccentric anomaly is  $E - e \sin E$ ; the Kepler equation (third Kepler law) implies, when the control is zero,

$$E - e \sin E = n t,$$

$t = 0$  being the time at the pericenter. Introducing (see for instance [4, sec. 3.6.3])

$$x_0 = (E - e \sin E)/n,$$

one has  $\frac{dx_0}{dt} = 1$  if  $u = 0$ . In the coordinates  $(x, x_0)$ , the system becomes

$$\frac{dx}{dt} = \sum_{i=1,2} u_i F'_i(x, x_0), \quad \frac{dx_0}{dt} = 1 + \sum_{i=1,2} u_i G_i(x, x_0).$$

Due to the implicit relation between  $E$  and  $x_0$ , the practical derivation of such equations is complicated, but they will be useful next to formally identify averaging with respect to  $l \in [0, 2\pi]$  and averaging with respect to  $t \in [0, 2\pi/n]$ .

We define the Hamiltonian lifts ( $i = 1, 2$ ):

$$H_i(x, p, l) = \langle p, F_i(x, p, l) \rangle, \quad H'_i(x, p, x_0) = \langle p, F'_i(x, p, x_0) \rangle. \quad (11)$$

**2.2. Averaging.** Using the previous equations and rescaling the control with  $u = \varepsilon v$  to introduce the small parameter, the trajectories parameterized by  $x_0$  are solutions of

$$\frac{dx}{dx_0} = \frac{\varepsilon \sum_{i=1,2} v_i F'_i(x, x_0)}{1 + \varepsilon \sum_{i=1,2} v_i G_i(x, x_0)},$$

which is approximated for small  $\varepsilon$  by

$$\frac{dx}{dx_0} = \varepsilon \sum_{i=1,2} v_i F'_i(x, x_0).$$

One considers the following minimization problems

- energy :  $Min_v \int_0^{x_0} \varepsilon^2 \sum_{i=1,2} v_i^2$
- time :  $Min_v x_0, \|v\| \leq 1$ .

Applying the Pontryagin maximum principle leads to the following respective Hamiltonians (normal case in the energy minimization problem),

$$\begin{aligned} H_e(x, p, x_0) &= \sum_{i=1,2} H'_i(x, p, x_0)^2 \\ H_t(x, p, x_0) &= \sqrt{\sum_{i=1,2} H'_i(x, p, x_0)^2} \end{aligned} \quad (12)$$

where  $H'_i$ , defined by (11), are periodic with respect to  $x_0$  with period  $2\pi/n$ .

*Remark 2.2.* In the single-input case (e.g. tangential thrust), there is a single term in the sums and one has, instead of (12):  $H_e = H'_1{}^2$ ,  $H_t = |H'_1|$ .

The respective averaged Hamiltonians (without confusion between notation) are

$$H_e(x, p) = \frac{n}{2\pi} \int_0^{2\pi/n} H_e(x, p, x_0) dx_0 \quad (13)$$

$$H_t(x, p) = \frac{n}{2\pi} \int_0^{2\pi/n} H_t(x, p, x_0) dx_0. \quad (14)$$

These may be re-computed in terms of  $H_1, H_2$  that have explicit expressions unlike  $H'_1, H'_2$ . Making the change of variables  $x_0 = \Xi(e, \omega, l)$  —with  $\Xi$  deduced from  $x_0 = (E - e \sin E)/n$ , (10) and (5)— in the integral, and using the fact that  $\partial \Xi / \partial l = 1/\Omega(x, l)$  and

$$H'_e(x, p, \Xi(e, \omega, l)) = H_e(x, p, l), H'_t(x, p, \Xi(e, \omega, l)) = H_t(x, p, l),$$

one gets, using (9),

$$H_e(x, p) = \frac{(1 - e^2)^{3/2}}{2\pi} \int_0^{2\pi} \left( \sum_{i=1,2} H_i(x, p, l)^2 \right) \frac{dl}{(1 + e \cos(l - \omega))^2} \quad (15)$$

$$H_t(x, p) = \frac{(1 - e^2)^{3/2}}{2\pi} \int_0^{2\pi} \sqrt{\sum_i H_i(x, p, l)^2} \frac{dl}{(1 + e \cos(l - \omega))^2}. \quad (16)$$

Observe that under some regularity assumptions [1] the averaged Hamiltonian system is associated to a Riemannian problem in the first case while the second case represents a non smooth Finsler problem, both defined by taking in the cotangent space the set of admissible velocities.

The non smoothness is related to averaging singularities of a control system that we explain next.

**Singularities.** Consider the time minimal control problem for a smooth system of the form

$$\frac{dx}{dt} = F_0(x) + \sum_{i=1,m} u_i F_i(x), \|u\| \leq 1.$$

Moreover assume for simplicity that the control distribution  $D = \text{span}\{F_1, \dots, F_m\}$  is involutive. From the maximum principle in the generic case the extremal control is defined by  $u_i = \frac{H_i(x, p)}{\sqrt{\sum_i H_i^2(x, p)}}$  where  $H_i(x, p)$  is the Hamiltonian lifts of  $F_i(x)$ .

More complicated extremals are related to the switching surface  $\Sigma : H_i = 0$ . Observe that in the single-input case the control is given by  $u_1 = \text{sign } H_1(x, p)$  and meeting the surface  $\Sigma$  transversally corresponds to a regular switching. This can be generalized to the multi-input case. More complicated singularities can occur in the non transversal case, for instance in relations with singular trajectories of the system (contained by definition in the surface).

### 3. THE ANALYSIS OF THE AVERAGED SYSTEMS FOR MINIMUM ENERGY

First of all we recall the results from the energy case [2]. The energy problem is taken as

$$\int_0^{l_f} \left( \sum_{i=1,2} u_i^2(t) + u_2^2(t) \right) dt \rightarrow \text{Min},$$

where we fix the final cumulated longitude  $l_f$  (it is slightly different from fixing the transfer time).

**3.1. The coplanar energy case.** In this case the quadratures to compute the averaged systems are explicit and we have the following proposition.

**Proposition 1.** *In the coordinates  $(n, e, \omega)$  the averaged Hamiltonian is up to a positive scalar given by*

$$H = \frac{1}{n^{5/3}} [18n^2 p_n^2 + 5(1 - e^2) p_e^2 + \frac{5 - 4e^2}{e^2} p_\omega^2] \quad (17)$$

where the singularity  $e = 0$  corresponds to circular orbits. In particular  $(n, e, \omega)$  are orthogonal coordinates for the Riemannian metric associated to  $H$  namely,

$$g = \frac{dn^2}{9n^{1/3}} + \frac{2n^{5/3} de^2}{5(1 - e^2)} + \frac{2n^{5/3} d\omega^2}{5 - 4e^2}.$$

Further normalizations are necessary to capture the main properties of the averaged orbital transfer.

**Proposition 2.** *In the elliptic domain we set*

$$r = \frac{2}{5} n^{5/6}, \varphi = \arcsin e$$

and the metric is isometric to

$$g = dr^2 + \frac{r^2}{c^2} (d\varphi^2 + G(\varphi) d\omega^2)$$

where  $c = \sqrt{2/5}$  and  $G(\varphi) = \frac{5 \sin^2 \varphi}{1 + 4 \cos^2 \varphi}$ .

**3.2. Transfer towards circular orbits.** As noticed in Remark 2.1, we may then ignore the cyclic variable  $\omega$  and allow negative  $e$ ; the elliptic domain is the  $\mathcal{X}$  given by (7).

The metric above then reduces to

$$g = dr^2 + r^2 d\psi^2, \quad \text{with } \psi = \varphi/c.$$

defined on the domain  $\{(r, \psi), 0 < r < +\infty, -\frac{\pi}{2c} < \psi < \frac{\pi}{2c}\}$ ; it is a polar metric isometric to the flat metric  $dx^2 + dz^2$  if we set  $x = r \sin \psi$  and  $z = r \cos \psi$ ; flatness can be checked in the original coordinates computing the Gauss curvature. We deduce the following theorem:

**Theorem 3.** *The geodesics of the averaged coplanar transfer towards circular orbits are straight lines in the domain  $\Sigma_0$  in suitable coordinates, namely*

$$x = \frac{2^{3/2}}{5} n^{5/6} \sin\left(\frac{1}{c} \arcsin e\right), z = \frac{2^{3/2}}{5} n^{5/6} \cos\left(\frac{1}{c} \arcsin e\right)$$

with  $c = \sqrt{2/5}$ . Since  $c < 1$ , the domain is not (geodesically) convex and the metric is not complete.

*Remark 3.1* (Tangential thrust). Those properties are still true when the thrust is only in the tangential direction except that the metric has a singularity at  $e = 1$ . The formulas are :

$$g = \frac{dn^2}{9n^{1/3}} + n^{5/3} \left[ \frac{1 + \sqrt{1 - e^2}}{4(1 - e^2)^{3/2}} de^2 + \frac{1 + \sqrt{1 - e^2}}{4(1 - e^2)} e^2 d\omega^2 \right]$$

and we slightly twist the previous coordinates using  $e = \sin \varphi \sqrt{1 + \cos^2 \varphi}$  to get the normal form  $dr^2 + (r^2/c_t)(d\varphi^2 + G_t(\varphi))$ ,  $c_t = c^2 = 2/5$ ,  $G_t(\varphi) = \sin^2 \varphi \left( \frac{1 - (1/2) \sin^2 \varphi}{1 - \sin^2 \varphi} \right)^2$ .

## 4. THE ANALYSIS OF THE AVERAGED SYSTEMS FOR MINIMUM TIME

**4.1. The Hamiltonian.** Let us compute  $H_t$  according to (16). The functions  $H_i$ ,  $i = 1, 2$  depends on  $n, e, \omega, p_n, p_e, p_\omega, l$ . Since we only consider transfer towards a circular orbit, we set  $p_\omega = 0$  and define  $h_1, h_2$  by

$$h_i(n, e, p_n, p_e, v) = H_i(n, e, \omega, p_n, p_e, 0, \omega + v) . \quad (18)$$

The right-hand side does not depend on the cyclic variable  $\omega$ , see Remark 2.1. From (4), and numbering the tangential and normal controls as 1,2, one gets:

$$h_1 = n^{-1/3} \left( -3n p_n \frac{\sqrt{1+2e \cos v + e^2}}{\sqrt{1-e^2}} + 2p_e \frac{(e + \cos v)\sqrt{1-e^2}}{\sqrt{1+2e \cos v + e^2}} \right) \quad (19a)$$

$$h_2 = -n^{-1/3} p_e \frac{\sin v (1-e^2)^{3/2}}{(1+e \cos v)\sqrt{1+2e \cos v + e^2}} \quad (19b)$$

Making the change of variable  $l = \omega + v$  in the integral in (16) ( $\omega$  does not vary in the integral; the integrand has period  $2\pi$  with respect to either  $l$  or  $v$ ), one obtains

$$H_t(n, e, p_n, p_e) = \frac{(1-e^2)^{3/2}}{2\pi} \int_0^{2\pi} \sqrt{\sum_i h_i(n, e, p_n, p_e, v)^2} \frac{dv}{(1+e \cos v)^2} . \quad (20)$$

**4.1.1. Full control case.** Here there are two terms in the sums. Taking as a new variable of integration the eccentric anomaly  $E$  defined by (10) (in particular,  $\frac{dv}{1+e \cos v} = (1-e \cos E)dE$ ), and making the change of variables

$$\rho \cos \psi = 3n p_n, \quad \rho \sin \psi = -\sqrt{1-e^2} p_e, \quad e = \sin \varphi \quad (21)$$

with  $-\frac{\pi}{2} < \varphi < \frac{\pi}{2}$  (but we sometimes continue to write  $e$  instead of  $\sin \varphi$  and  $\sqrt{1-e^2}$  instead of  $\cos \varphi$  for short), one has

$$H_t(n, \sin \varphi, \frac{\rho \cos \psi}{3n}, \frac{-\rho \sin \psi}{\cos \varphi}) = \rho n^{1/3} L(\psi, \varphi) \quad (22)$$

with

$$L(\psi, \varphi) = \frac{1}{2\pi} \int_0^{2\pi} \sqrt{\tilde{I}(\varphi, \psi, E)} dE, \quad (23)$$

$$\begin{aligned} \tilde{I}(\varphi, \psi, E) &= \alpha^{1,1}(\varphi, \cos E) \cos^2 \psi \\ &\quad + 2 \alpha^{1,2}(\varphi, \cos E) \cos \psi \sin \psi + \alpha^{2,2}(\varphi, \cos E) \sin^2 \psi \end{aligned} \quad (24)$$

with

$$\begin{aligned} \alpha^{1,1} &= 1 - \sin^2 \varphi \cos^2 E, & \alpha^{1,2} &= -2 \cos \varphi (1 - \sin \varphi \cos E) \cos E, \\ \alpha^{2,2} &= (1 - \sin \varphi \cos E) (1 - 3 \sin \varphi \cos E + 3 \cos^2 E - \sin \varphi \cos^3 E) \end{aligned} \quad (25)$$

**4.1.2. Tangential thrust.** Here only the tangential component of the control is nonzero, hence  $H_2$  is replaced by zero, see remark 2.2. Denoting by  $H_t^1$  the Hamiltonian for the tangential thrust case, (20) is replaced by

$$H_t^1(n, e, p_n, p_e) = \frac{(1-e^2)^{3/2}}{2\pi} \int_0^{2\pi} |h_i(n, e, p_n, p_e, v)| \frac{dv}{(1+e \cos v)^2} . \quad (26)$$

Taking again the eccentric anomaly  $E$  as a new variable of integration and in the same coordinates  $(\psi, \varphi, n, \rho)$  defined by (21), one has

$$H_t^1(n, \sin \varphi, \frac{\rho \cos \psi}{3n}, \frac{-\rho \sin \psi}{\cos \varphi}) = \rho n^{1/3} M(\psi, \varphi) \quad (27)$$

with

$$M(\psi, \varphi) = \frac{1}{2\pi} \int_0^{2\pi} |\tilde{J}(\varphi, \psi, E)| dE, \quad (28)$$

$$\tilde{J}(\varphi, \psi, E) = -\sqrt{\frac{1 - e \cos E}{1 + e \cos E}} ((\sin \varphi \cos \psi - 2 \cos \varphi \sin \psi) \cos E + \cos \psi). \quad (29)$$

**4.2. Singularities of the Hamiltonian in the single-input and two-input cases.** We give results on smoothness of the Hamiltonians, both in the full control and in the tangential thrust case. Studying more precisely these singularities are an interesting program that is not yet carried, we only give the location of the points where these are not smooth (but still  $C^1$ ) and a result on the modulus of continuity of the differential (which is important because it is the right-hand side of the Hamiltonian equation).

4.2.1. *Full control case.* From (22),  $H_t$  is as smooth as  $L : \mathcal{C} \rightarrow \mathbb{R}$ , where

$$\mathcal{C} = \{(\psi, \varphi), \psi \in (\mathbb{R}/2\pi\mathbb{Z}), \varphi \in \mathbb{R}, -\frac{\pi}{2} < \varphi < \frac{\pi}{2}\} = \mathbb{R}/2\pi\mathbb{Z} \times (-\frac{\pi}{2}, \frac{\pi}{2}). \quad (30)$$

**Proposition 4.** *The map  $L : \mathcal{C} \rightarrow \mathbb{R}$  is real analytic away from*

$$\mathcal{S} = \{(\psi, \varphi), \tan \psi = \frac{\cos \varphi}{2(1 - \sin \varphi)}\} \cup \{(\psi, \varphi), \tan \psi = -\frac{\cos \varphi}{2(1 + \sin \varphi)}\}. \quad (31)$$

*It is everywhere continuously differentiable, and in a neighborhood of a point  $\xi = (\psi, \varphi) \in \mathcal{S}$ , its differential satisfies*

$$\|DL(\xi + \delta) - DL(\xi)\| \leq k \|\delta\| \ln(1/\|\delta\|) \quad (32)$$

for some constant  $k > 0$ .

*Proof.* When  $(\psi, \varphi)$  is outside  $\mathcal{S}$ ,  $\tilde{I}$  vanishes for no  $E$ , hence smoothness is obvious. The degree of regularity at points in  $\mathcal{S}$  is given in [1].  $\square$

4.2.2. *Tangential thrust.* From (27),  $H_t^1$  is as smooth as  $M : \mathcal{C} \rightarrow \mathbb{R}$ .

**Proposition 5.** *The map  $M : \mathcal{C} \rightarrow \mathbb{R}$  is real analytic away from*

$$\mathcal{S}' = \{(\psi, \varphi), \tan \psi = \frac{1}{2}(-\sin \varphi - 1)\} \cup \{(\psi, \varphi), \tan \psi = \frac{1}{2}(-\sin \varphi + 1)\}. \quad (33)$$

*It is everywhere continuously differentiable, and its differential is Hölder with exponent  $1/2$ .*

*Proof.*  $\mathcal{S}'$  is the frontier between the open set where  $\tilde{I}$  vanishes for two values of  $E$  and the open region where it does not vanish for any  $E$ . It is easy to prove that it is analytic in both region. The surface  $\mathcal{S}'$  is not a type of singularities studied in [1]; a standard computation shows that  $M$  is the patch of two functions, one of them has a real analytic continuation through  $\mathcal{S}'$  while the other one has second derivatives that tend to infinity and in fact the differential is no more than Hölder.  $\square$

*We give no further results on the tangential thrust case in this paper.*

**4.3. The Hamiltonian flow in the full control case.** We shall further study the solutions of the Hamiltonian equation

$$\dot{n} = \frac{\partial H_t}{\partial p_n}, \quad \dot{e} = \frac{\partial H_t}{\partial p_e}, \quad \dot{p}_n = -\frac{\partial H_t}{\partial n}, \quad \dot{p}_e = -\frac{\partial H_t}{\partial e} \quad (34)$$

in the coordinates  $(n, \varphi, \psi, \rho)$ .

**Proposition 6.** *In the coordinates  $(n, \varphi, \psi, \rho)$  defined by (21), and after the change of time*

$$dt = n^{-1/3} d\tau, \quad (35)$$

equations (34) yield (lower indices stand for partial derivatives):

$$d\psi/d\tau = -L(\psi, \varphi) \sin \psi - L_\varphi(\psi, \varphi) \cos \psi, \quad (36a)$$

$$d\varphi/d\tau = L(\psi, \varphi) \sin \psi + L_\psi(\psi, \varphi) \cos \psi, \quad (36b)$$

$$dn/d\tau = -3n(L(\psi, \varphi) \cos \psi - L_\psi(\psi, \varphi) \sin \psi), \quad (36c)$$

$$\text{and } \rho \text{ is given by: } \quad \rho(\tau) = \rho(0) \left( \frac{n(0)}{n(\tau)} \right)^{1/3} \frac{L(\psi(0), \varphi(0))}{L(\psi(\tau), \varphi(\tau))}. \quad (37)$$

The “time”  $\tau$  is related to the real time  $t$  by

$$t = \frac{n(\tau)^{-1/3} \cos \psi(\tau)}{L(\varphi(\tau), \psi(\tau))} - \frac{n(0)^{-1/3} \cos \psi(0)}{L(\varphi(0), \psi(0))}. \quad (38)$$

The evolution of  $\rho$  is not important in the sequel.

*Proof.* Differentiating (21) and using (34) yields:

$$\begin{aligned} \dot{\psi} &= \frac{1}{\rho} \left( 3n \sin \psi \frac{\partial H_t}{\partial n} + \cos \varphi \cos \psi \frac{\partial H_t}{\partial e} \right) - \cos \psi \sin \psi \left( \frac{1}{n} \frac{\partial H_t}{\partial p_n} + \frac{\sin \varphi}{\cos^2 \varphi} \frac{\partial H_t}{\partial p_e} \right), \\ \dot{\varphi} &= \frac{1}{\cos \varphi} \frac{\partial H_t}{\partial p_e}, \quad \dot{n} = \frac{\partial H_t}{\partial p_n}. \end{aligned} \quad (39)$$

Differentiating (22) with respect to  $n, \varphi, \rho, \psi$  and solving for  $\frac{\partial H_t}{\partial n}, \frac{\partial H_t}{\partial e}, \frac{\partial H_t}{\partial p_n}, \frac{\partial H_t}{\partial p_e}$  yields these quantities as linear combinations of  $L(\psi, \varphi), L_\varphi(\psi, \varphi), L_\psi(\psi, \varphi)$  with coefficients depending on  $n, \varphi, \rho, \psi$ ; substituting these expressions in (39), one gets:

$$\begin{aligned} \dot{\psi} &= n^{1/3} (-L \sin \psi - L_\varphi \cos \psi), \\ \dot{\varphi} &= n^{1/3} (L \sin \psi + L_\psi \cos \psi), \\ \dot{n} &= -3n^{4/3} (L \cos \psi - L_\psi \sin \psi). \end{aligned}$$

If we define a new time  $\tau$  by (35), we do get (36). These equations imply

$$\frac{d}{d\tau} \left( \frac{n^{-1/3} \cos \psi}{L(\psi, \varphi)} \right) = n^{-1/3}, \text{ and relation (38) follows.} \quad \square$$

Equation (36) reads  $d\psi/d\tau = a(\psi, \varphi)$ ,  $d\varphi/d\tau = b(\psi, \varphi)$ ,  $dn/d\tau = -3nc(\psi, \varphi)$  with

$$a(\psi, \varphi) = -L(\psi, \varphi) \sin \psi - L_\varphi(\psi, \varphi) \cos \psi, \quad (40a)$$

$$b(\psi, \varphi) = L(\psi, \varphi) \sin \psi + L_\psi(\psi, \varphi) \cos \psi, \quad (40b)$$

$$c(\psi, \varphi) = L(\psi, \varphi) \cos \psi - L_\psi(\psi, \varphi) \sin \psi. \quad (40c)$$

It is a differential equation in the three variables

$$(\psi, \varphi, n) \in \mathcal{C} \times (0, +\infty), \quad (41)$$

where  $\mathcal{C}$  is the cylinder (30), with the nice feature that (36a)-(36b) form an autonomous system of equations in the two variables  $(\psi, \varphi) \in \mathcal{C}$ , that we analyze in section 4.4, while the last equation translates into

$$n(\tau) = n(0) \exp\left(-3 \int_0^\tau c(\psi(\sigma), \varphi(\sigma)) d\sigma\right). \quad (42)$$

Let us give two preliminary results. The first one states invariance of equation (36) under the transformations  $(\psi, \varphi, n, \tau) \mapsto (-\psi, -\varphi, n, \tau)$  and  $(\psi, \varphi, n, \tau) \mapsto (-\tau, \pi + \psi, n, \tau)$ , and the second one describes the variations of the functions  $b, c$ .

**Proposition 7** (Symmetries). *If  $\tau \mapsto (\psi(\tau), \varphi(\tau))$  is a solution of (36a)-(36b) defined on the time interval  $[0, \tau_{\text{fin}}]$ , then  $\tau \mapsto (\psi^\sharp(\tau), \varphi^\sharp(\tau))$  and  $\tau \mapsto (\psi^+(\tau), \varphi^+(\tau))$  with*

$$\begin{aligned} \psi^\sharp(\tau) &= -\psi(\tau), & \psi^+(\tau) &= \psi(\tau_{\text{fin}} - \tau) + \pi, \\ \varphi^\sharp(\tau) &= -\varphi(\tau), & \varphi^+(\tau) &= \varphi(\tau_{\text{fin}} - \tau), \end{aligned} \quad (43)$$

are also solutions of (36a)-(36b) on the same time interval  $[0, \tau_{\text{fin}}]$  and they satisfy

$$\int_0^{\tau_{\text{fin}}} c(\psi^\sharp(\tau), \varphi^\sharp(\tau)) d\tau = \int_0^{\tau_{\text{fin}}} c(\psi^+(\tau), \varphi^+(\tau)) d\tau = \int_0^{\tau_{\text{fin}}} c(\psi(\tau), \varphi(\tau)) d\tau. \quad (44)$$

We also use the “ $\sharp$ ” and “+” notation to denote the transformations  $(\psi, \varphi) \mapsto (-\psi, -\varphi)$  and  $(\psi, \varphi) \mapsto (-\tau, \pi + \psi)$  in the variables  $\varphi, \psi$ .

*Proof.* This is a straightforward consequence of the following relations, that may be derived from the expression of  $a, b, c$ :

$$\begin{aligned} a(\psi + \pi, \varphi) &= -a(\psi, \varphi), & a(-\psi, -\varphi) &= -a(\psi, \varphi), \\ b(\psi + \pi, \varphi) &= -b(\psi, \varphi), & b(-\psi, -\varphi) &= -b(\psi, \varphi), \\ c(\psi + \pi, \varphi) &= -c(\psi, \varphi), & c(-\psi, -\varphi) &= c(\psi, \varphi). \end{aligned} \quad (45) \quad \square$$

**Lemma 8** (Sign and variations of  $b$  and  $c$ ). *For fixed  $\varphi$ ,*

- the function  $b$  is maximum for  $\psi = \frac{\pi}{2}$  and minimum for  $\psi = -\frac{\pi}{2}$ , it increases strictly with  $\psi$  when  $-\frac{\pi}{2} < \psi < \frac{\pi}{2}$  and decreases when  $\frac{\pi}{2} < \psi < \frac{3\pi}{2}$ ,
- the function  $c$  is maximum for  $\psi = 0$  and minimum for  $\psi = \pi$ , it decreases strictly with  $\psi$  when  $0 < \psi < \pi$  and increases when  $\pi < \psi < 2\pi$ .

There exists two continuous maps  $Z^b$  and  $Z^c : [-\frac{\pi}{2}, \frac{\pi}{2}] \rightarrow \mathbb{R}/2\pi\mathbb{Z}$ , such that

$$b(\psi, \varphi) = 0 \Leftrightarrow \left(\psi = Z^b(\varphi) \text{ or } \psi = Z^b(\varphi) + \pi\right), \quad (46)$$

$$c(\psi, \varphi) = 0 \Leftrightarrow \left(\psi = Z^c(\varphi) \text{ or } \psi = Z^c(\varphi) + \pi\right). \quad (47)$$

They satisfy

$$Z^b(-\frac{\pi}{2}) = Z^b(0) = Z^b(\frac{\pi}{2}) = 0, \quad Z^c(-\frac{\pi}{2}) = Z^c(0) = Z^c(\frac{\pi}{2}) = \frac{\pi}{2}, \quad (48)$$

$$\frac{\partial Z^b}{\partial \varphi}(0) = -2, \quad (49)$$

and their graphs lie in the stripes  $-\frac{\pi}{8} < \psi < \frac{\pi}{8}$  and  $\frac{7\pi}{16} < \psi < \frac{9\pi}{16}$  respectively:

$$\begin{aligned} -\frac{\pi}{2} < \varphi < 0 &\Rightarrow 0 < Z^b(\varphi) < \frac{\pi}{8}, & -\frac{\pi}{2} < \varphi < 0 &\Rightarrow \frac{\pi}{2} < Z^c(\varphi) < \frac{9\pi}{16}, \\ 0 < \varphi < \frac{\pi}{2} &\Rightarrow -\frac{\pi}{8} < Z^b(\varphi) < 0, & 0 < \varphi < \frac{\pi}{2} &\Rightarrow \frac{7\pi}{16} < Z^c(\varphi) < \frac{\pi}{2}. \end{aligned} \quad (50)$$

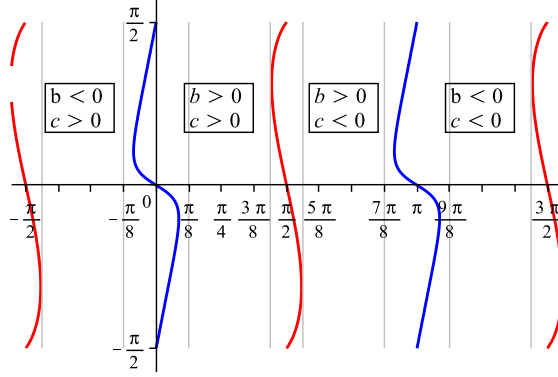


FIGURE 1. The sign of  $\dot{\psi} = b(\psi, \varphi)$  and  $\dot{\lambda} = c(\psi, \varphi)$ . The curves are, from left to right ( $\psi = -\frac{\pi}{2}$  is identified with  $\psi = \frac{3\pi}{2}$ ):  $\psi = Z^c(\varphi) + \pi$ ,  $\psi = Z^b(\varphi)$ ,  $\psi = Z^c(\varphi)$ ,  $\psi = Z^b(\varphi) + \pi$  and  $\psi = Z^c(\varphi) + \pi$  again.

*Proof.* The derivatives of  $b$  and  $c$  with respect to  $\psi$  are given by

$$\frac{\partial b}{\partial \psi}(\psi, \varphi) = \frac{\cos \psi}{\pi} \int_0^\pi \frac{(1 - \sin^2 \varphi \cos^2 E)^4 \sin^2 E}{\tilde{I}(\psi, \varphi, E)^{3/2}} dE, \quad (51)$$

$$\frac{\partial c}{\partial \psi}(\psi, \varphi) = \frac{-\sin \varphi}{\pi} \int_0^\pi \frac{(1 - \sin^2 \varphi \cos^2 E)^4 \sin^2 E}{\tilde{I}(\psi, \varphi, E)^{3/2}} dE. \quad (52)$$

This accounts for the very first part of the lemma.

The values of  $b$  and  $c$  for  $\varphi = 0$  and  $\varphi = \frac{\pi}{2}$  respectively are given by

$$b(0, \varphi) = \frac{2 \cos \varphi \sin \varphi}{\pi} \int_0^\pi \frac{\cos^2 E dE}{\sqrt{1 - \sin^2 \varphi \cos^2 E}}, \quad (53)$$

$$c\left(\frac{\pi}{2}, \varphi\right) = \frac{-2 \cos \varphi}{\pi} \int_0^\pi \sqrt{\frac{1 - \sin \varphi \cos E}{1 - 3 \sin \varphi \cos E + 3 \cos^2 E - \sin \varphi \cos^3 E}} \cos E dE. \quad (54)$$

Both right-hand sides have the same sign as  $\sin \varphi$  (obvious in (53); in (54), compare the values of the integrand for  $E$  and  $\pi - E$ ); hence both  $b(0, \varphi)$  and  $c(\frac{\pi}{2}, \varphi)$  are negative between  $-\frac{\pi}{2}$  and 0, positive between 0 and  $\frac{\pi}{2}$  and zero at 0 (and  $\pm\frac{\pi}{2}$ , but this is out of  $\mathcal{C}$ ); this implies existence of  $Z^b$  and  $Z^c$  satisfying (46), (47) and (48) (recall that  $b(\psi + \pi, \varphi) = -b(\psi, \varphi)$ ,  $c(\psi + \pi, \varphi) = -c(\psi, \varphi)$ ). The relation (49) follows from (56). The values  $\frac{\pi}{8}$  and  $\frac{\pi}{16}$  were obtained numerically, see the plot in figure 1.  $\square$   $\square$

**4.4. study of the 2-D system.** We now study the differential equation

$$\dot{\psi} = a(\psi, \varphi), \quad \dot{\varphi} = b(\psi, \varphi) \quad (55)$$

on the cylinder  $\mathcal{C}$  (see (30)), with  $a, b$  given by (40), (23), (24), (25).

**Lemma 9.** *For each  $(\psi^\circ, \varphi^\circ) \in \mathcal{C}$ , there is a unique solution to (55) such that  $(\psi(0), \varphi(0)) = (\psi^\circ, \varphi^\circ)$ , defined on a maximum interval of definition  $(\tau^-, \tau^+)$  where either  $\tau^- = -\infty$  or  $\varphi(\tau^-) = \pm\frac{\pi}{2}$ , and either  $\tau^+ = +\infty$  or  $\varphi(\tau^+) = \pm\frac{\pi}{2}$ . The flow is real analytic on any domain that does not intersect  $\mathcal{S}$  (see (31)).*

*Proof.* As seen in [1], the degree of smoothness displayed in Proposition 4 suffices to ensure existence uniqueness of solutions to the Cauchy problem.  $\square$

**Lemma 10.** *The differential equation (55) has two equilibrium points on  $\mathcal{C}$ , located at  $(0, 0)$  and  $(\pi, 0)$ .*

*Proof.* From Lemma 8,  $b$  vanishes only on the curves  $\psi = Z^b(\varphi)$  and  $\psi = Z^b(\varphi) + \pi$ ,  $-\frac{\pi}{2} < \varphi < \frac{\pi}{2}$ . The fact that  $b(\varphi, Z^b(\varphi))$  vanishes only when  $\varphi = 0$  was determined numerically.  $\square$

**Lemma 11.** *The equilibrium points on  $(0, 0)$  and  $(\pi, 0)$  are hyperbolic saddle points with linearization  $\begin{pmatrix} -2 & 1/2 \\ 1/2 & 1 \end{pmatrix}$  at  $(0, 0)$  and  $-\begin{pmatrix} -2 & 1/2 \\ 1/2 & 1 \end{pmatrix}$  at  $(\pi, 0)$ .*

*Proof.* An easy computation shows that

$$\frac{\partial a}{\partial \psi}(0, 0) = -2, \quad \frac{\partial a}{\partial \varphi}(0, 0) = \frac{1}{2}, \quad \frac{\partial b}{\partial \psi}(0, 0) = \frac{1}{2}, \quad \frac{\partial b}{\partial \varphi}(0, 0) = 1. \quad \square \quad (56)$$

This guarantees the existence of local stable and unstable manifolds of the two equilibria, tangent to the eigenvectors of the linearization at these points. The following is a global description of these manifolds, made of the only (four) solutions that tend to one of these points, in positive and negative time respectively:

**Lemma 12** (Stable and unstable manifolds). *1. There are continuously differentiable maps  $S^0$  and  $U^0$ ,  $(-\frac{\pi}{2}, \frac{\pi}{2}) \rightarrow \mathbb{R}/2\pi\mathbb{Z}$ , such that the stable and unstable manifolds of  $(0, 0)$  are, respectively,*

$$\begin{aligned} S^0 &= \{(\psi, \varphi), \psi = S^0(\varphi), -\frac{\pi}{2} < \varphi < \frac{\pi}{2}\} \\ \text{and } U^0 &= \{(\psi, \varphi), \psi = U^0(\varphi), -\frac{\pi}{2} < \varphi < \frac{\pi}{2}\}. \end{aligned} \quad (57)$$

The maps  $S^0, U^0$  satisfy:

$$\begin{aligned} S^0(0) = U^0(0) &= 0, \quad \frac{\partial U^0}{\partial \varphi}(0) = \sqrt{10} - 3, \quad \frac{\partial S^0}{\partial \varphi}(0) = -\sqrt{10} - 3 \\ S^0(-\varphi) &= -S^0(\varphi), \quad U^0(-\varphi) = -U^0(\varphi), \end{aligned} \quad (58)$$

*2. The stable and unstable manifolds of  $(\pi, 0)$  are*

$$\begin{aligned} S^\pi &= \{(\psi, \varphi), \psi = S^\pi(\varphi), -\frac{\pi}{2} < \varphi < \frac{\pi}{2}\} \\ \text{and } U^\pi &= \{(\psi, \varphi), \psi = U^\pi(\varphi), -\frac{\pi}{2} < \varphi < \frac{\pi}{2}\} \end{aligned} \quad (59)$$

with

$$S^\pi(\varphi) = \pi + U^0(\varphi), \quad U^\pi(\varphi) = \pi + S^0(\varphi). \quad (60)$$

*3. The following inequalities give the position of the stable and unstable manifolds (pictured on figure 4) with respect to the curves  $\psi = Z^b(\varphi)$  and  $\psi = Z^c(\varphi)$  where  $b$  and  $c$  vanish (see Lemma 8):*

$$\begin{aligned} \varphi < 0 &\Rightarrow -\frac{\pi}{2} < U^0(\varphi) < Z^b(\varphi) < 0 < S^0(\varphi) < \frac{\pi}{2} < Z^c(\varphi) < S^\pi(\varphi), \\ \varphi > 0 &\Rightarrow -\frac{\pi}{2} < S^0(\varphi) < 0 < Z^b(\varphi) < U^0(\varphi) < Z^c(\varphi) < \frac{\pi}{2} < U^\pi(\varphi). \end{aligned} \quad (61)$$

*Proof.* Point 2 is an immediate consequence of Point 1 and the the “+” symmetry in Lemma 7. Let us go on with points 1 and 3.

The linearization at  $(0, 0)$  is, according to Lemma 11,  $\begin{pmatrix} -2 & 1/2 \\ 1/2 & 1 \end{pmatrix}$ . It has

$$\begin{aligned} &\text{a positive eigenvalue } (\sqrt{10} - 1)/2 \text{ with eigenvector } (\sqrt{10} - 3, 1), \\ &\text{a negative eigenvalue } -(\sqrt{10} + 1)/2 \text{ with eigenvector } (-\sqrt{10} - 3, 1). \end{aligned} \quad (62)$$

*Unstable manifold.* It is made of the equilibrium  $(0, 0)$  and two solutions that go to  $(0, 0)$  as time goes to  $-\infty$ . According to (62), they are both tangent to the line  $\{\psi = (\sqrt{10} - 3)\varphi\}$  at  $(0, 0)$ ; one of them approaches with positive  $\psi$  and  $\varphi$  and the other one with negative  $\psi$  and  $\varphi$ ; we only consider the first one and call it  $\tau \mapsto (\bar{\psi}(\tau), \bar{\varphi}(\tau))$ , defined on the time interval  $(-\infty, \bar{\tau}^+)$ ,  $\bar{\tau}^+ \leq +\infty$ ; the result for the other one follows by symmetry. On the one hand, we have  $\lim_{\tau \rightarrow -\infty} \bar{\psi}(\tau) = \lim_{\tau \rightarrow -\infty} \bar{\varphi}(\tau) = 0$ ,  $\lim_{\tau \rightarrow -\infty} (\dot{\bar{\psi}}(\tau)/\dot{\bar{\varphi}}(\tau)) = \sqrt{10} - 3$  and  $\bar{\psi}(\tau) > 0$ ,  $\bar{\varphi}(\tau) > 0$  for  $\tau$  close enough to  $-\infty$ ; since  $1/16 < \sqrt{10} - 3 < 1/5$ , this implies that  $(\bar{\psi}(\tau), \bar{\varphi}(\tau))$  is in the domain  $\{\varphi/16 < \psi < \varphi/5, \varphi > 0\}$  for all  $\tau$  in  $(-\infty, \bar{\tau}]$  for some negative large enough  $\bar{\tau}$ . On the other hand, that domain is positively invariant (i.e. a solution that is in this domain at some time is also in this domain for any larger time) for the differential equation (55) on  $\mathcal{C}$  because (numerical evidence, see figure 2):

$$\frac{a(\varphi/16, \varphi) - b(\varphi/16, \varphi)/16}{\varphi} > 0 \quad \text{and} \quad \frac{a(\varphi/5, \varphi) - b(\varphi/5, \varphi)/5}{\varphi} < 0 \quad (63)$$

for all  $\varphi$  in  $[0, \pi/2]$ . Hence  $(\bar{\psi}(\tau), \bar{\varphi}(\tau))$  is in this domain for all  $\tau$  in  $(-\infty, \bar{\tau}^+)$ .

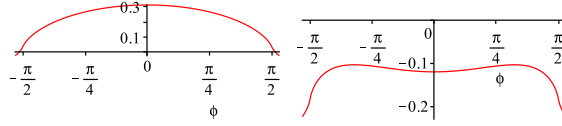


FIGURE 2. Left:  $\frac{1}{\varphi} (a(\varphi/16, \varphi) - b(\varphi/16, \varphi)/16)$ ;  
right:  $\frac{1}{\varphi} (a(\varphi/5, \varphi) - b(\varphi/5, \varphi)/5)$

If  $\bar{\tau}^+ < +\infty$ , the solution cannot stay in a compact subset of the domain, hence  $\lim_{\tau \rightarrow \bar{\tau}^+} \varphi(\tau) = \pi/2$ ; if  $\bar{\tau}^+ = +\infty$ , since, according to Lemma 8,  $\dot{\varphi}$  is positive in this domain,  $\bar{\varphi}(\tau)$  tends to a limit and  $\dot{\bar{\varphi}}(\tau)$  tends to zero as  $\tau \rightarrow +\infty$ ; this would imply that the solution  $(\bar{\psi}(\tau), \bar{\varphi}(\tau))$  tends to  $(0, 0)$  because, again from Lemma 8, the only point in the topological closure of the domain where  $\dot{\varphi} = 0$  is the origin; but  $\varphi(\tau)$  cannot tend to zero as  $\tau \rightarrow +\infty$  because it is positive for some time and is strictly increasing. Hence  $\bar{\varphi}(\tau)$  is defined for  $-\infty < \tau < \bar{\tau}^+ < +\infty$ ,  $\lim_{\tau \rightarrow -\infty} \bar{\varphi}(\tau) = 0$ ,  $\lim_{\tau \rightarrow \bar{\tau}^+} \bar{\varphi}(\tau) = \pi/2$  and  $d\bar{\varphi}/d\tau > 0$ , hence the parameterized curve  $\tau \mapsto (\bar{\psi}(\tau), \bar{\varphi}(\tau))$  is a graph  $\psi = U^0(\varphi)$ ,  $0 < \varphi < \pi/2$ . This  $U^0$  obviously satisfies the properties of points 1 and 3.

*Stable manifold.* It is made of the equilibrium  $(0, 0)$  and two solutions that go to  $(0, 0)$  as time goes to  $+\infty$ . According to (62), they are both tangent to the line  $\{\psi = -(\sqrt{10} + 3)\varphi\}$  at the origin. Since the slope is negative, one solution approaches with positive  $\psi$  and negative  $\varphi$  and the other one negative  $\psi$  and positive  $\varphi$ ; we only consider the first one and call it  $\tau \mapsto (\bar{\psi}(\tau), \bar{\varphi}(\tau))$ ; the result for the other one follows by symmetry.

Define the continuous piecewise affine map  $z : [-\pi/2, 0] \rightarrow [-\pi/2, 0]$  by

$$z(\varphi) = \begin{cases} -2\varphi & \text{if } -\frac{3}{64}\pi \leq \varphi \leq 0 \\ \frac{21}{256}\pi - \frac{1}{4}\varphi & \text{if } -\frac{11}{64}\pi \leq \varphi - \frac{3}{64}\pi \\ \pi/8 & \text{if } \varphi \leq -\frac{11}{64}\pi \end{cases}$$

The curve  $\psi = z(\varphi)$  is depicted on Figure 3. Consider the domain

$$\mathcal{D} = \{(\psi, \varphi), z(\varphi) < \psi < \pi + U^0(\varphi), \varphi < 0\} \subset \mathcal{C}.$$

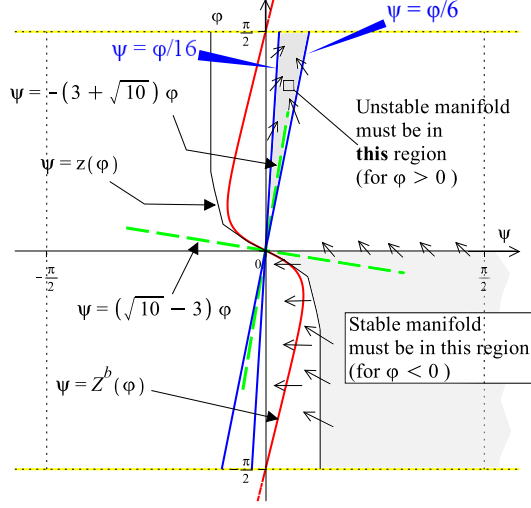


FIGURE 3. Illustration of the proof of Lemma 12.

It is negatively invariant (if a solution is in it for some time, it is in it for all *smaller* times) because:

- according to Lemma 8,  $\varphi = 0$  and  $0 < \psi < \pi \Rightarrow \dot{\varphi} > 0$ ,
- we just proved that  $\psi = U^0(\varphi)$  is an invariant manifold, and so is  $\psi = \pi + U^0(\varphi)$  by symmetry (Lemma 7),
- the derivative of  $\psi - z(\varphi)$  along solutions at a point where  $\psi = z(\varphi)$ ,  $\pi/2 < \varphi < 0$ , is negative: it can be checked numerically that

$$\begin{aligned} -3\pi/64 \leq \varphi \leq 0 &\Rightarrow a(-2\varphi, \varphi) + 2b(-2\varphi, \varphi) < 2\varphi, \\ -11\pi/64 \leq \varphi \leq -3\pi/64 &\Rightarrow a(\frac{21}{256}\pi - \varphi/4, \varphi) + \frac{1}{4}b(\frac{21}{256}\pi - \varphi/4, \varphi) < -1/10, \\ -\pi/2 \leq \varphi \leq -11\pi/64 &\Rightarrow a(\pi/8, \varphi) < -1/10 \end{aligned}$$

(the last inequality is even true for all  $\varphi$  in  $[-\pi/2, 0]$ ). We have  $\lim_{\tau \rightarrow +\infty} \bar{\psi}(\tau) = \lim_{\tau \rightarrow +\infty} \bar{\varphi}(\tau) = 0$ ,  $\lim_{\tau \rightarrow +\infty} (\dot{\bar{\psi}}(\tau)/\dot{\bar{\varphi}}(\tau)) = -(\sqrt{10} + 3)$  and  $\bar{\psi}(\tau) > 0$ ,  $\bar{\varphi}(\tau) < 0$  for  $\tau$  large enough, hence  $(\bar{\psi}(\tau), \bar{\varphi}(\tau)) \in \mathcal{D}$  for  $\tau$  large enough; since  $\mathcal{D}$  is negatively invariant, this implies  $(\bar{\psi}(\tau), \bar{\varphi}(\tau)) \in \mathcal{D}$  for all  $\tau$  in the maximal interval of definition of the solution. If the solution was defined for all positive or negative time, then, since  $\dot{\varphi} > 0$  on  $\mathcal{D}$ ,  $\bar{\varphi}(\tau)$  would have a limit as  $\tau \rightarrow -\infty$ , but this is absurd because  $\dot{\varphi} = b(\psi, \varphi)$  has a strictly positive lower bound on any  $\{(\psi, \varphi) \in \mathcal{D}, \varphi = \text{constant}\}$  for any negative constant larger than  $-\pi/2$ . Hence there is a  $\bar{\tau}$  such that the solution remains in  $\mathcal{D}$  when  $\bar{\tau} < \tau < +\infty$  and  $\lim_{\tau \rightarrow \bar{\tau}^-} \bar{\varphi}(\tau) = -\pi/2$ . This and the fact that  $\dot{\varphi}$  is positive implies that the trajectory defines a graph  $\psi = S^0(\varphi)$ ,  $-\pi/2 < \varphi < 0$ . The function  $S^0$  obviously has the properties of points 1 and 3 (the comparison with  $Z^b$  allows from the solution being contained in  $\mathcal{D}$  because  $Z^b(\varphi) < z(\varphi)$  for negative  $\varphi$ ).  $\square$

The stable and unstable manifolds  $S^0, U^0, S^\pi, U^\pi$ , that intersect at the equilibria  $(0, 0)$  and  $(\pi, 0)$  are invariant sets that divide the cylinder  $\mathcal{C}$  into six open regions:

$$F = \{(\psi, \varphi), -\frac{\pi}{2} < \varphi < 0 \text{ and } U^0(\varphi) < \psi < S^0(\varphi)\},$$

$$\begin{aligned}
 F^+ &= \{(\psi, \varphi), -\frac{\pi}{2} < \varphi < 0 \text{ and } S^\pi(\varphi) < \psi < U^\pi(\varphi)\}, \\
 F^\sharp &= \{(\psi, \varphi), 0 < \varphi < \frac{\pi}{2} \text{ and } S^0(\varphi) < \psi < U^0(\varphi)\}, \\
 F^{\sharp+} &= \{(\psi, \varphi), 0 < \varphi < \frac{\pi}{2} \text{ and } U^\pi(\varphi) < \psi < S^\pi(\varphi)\}, \\
 E &= \{(\psi, \varphi), S^0(\varphi) < \psi < S^\pi(\varphi) \text{ if } \varphi \leq 0, \\
 &\quad U^0(\varphi) < \psi < U^\pi(\varphi) \text{ if } \varphi \geq 0\}, \\
 E^+ &= \{(\psi, \varphi), U^\pi(\varphi) < \psi < U^0(\varphi) \text{ if } \varphi \leq 0, \\
 &\quad S^\pi(\varphi) < \psi < S^0(\varphi) \text{ if } \varphi \geq 0\}.
 \end{aligned}$$

$E$  is self-symmetric for the “ $\sharp$ ” symmetry and  $E^+$  is its image by the “ $+$ ” symmetry;  $F^+$ ,  $F^\sharp$ ,  $F^{\sharp+}$  are the images of  $F$  by the “ $\sharp$ ” and “ $+$ ” symmetries, see Lemma 7.

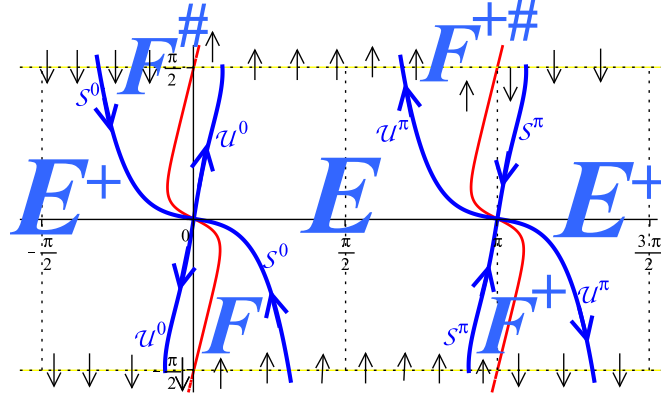


FIGURE 4. Six invariant regions separated by the stable and unstable manifolds of  $(0, 0)$  and  $(\pi, 0)$ . The other curves are  $\psi = Z^b(\varphi)$  and  $\psi = \pi + Z^b(\varphi)$ , where  $b(\psi, \varphi)$  changes sign.

**N.B.:** The stable and unstable manifolds as drawn on this picture are “artist views”, no computation of the actual stable and unstable manifolds were done besides the estimations of Lemma 12.

**4.5. geodesic convexity.** The above results allow us to prove geodesic convexity of the elliptic domain  $\mathcal{X}$  (see (7)).

**Theorem 13** (geodesic convexity). *For any  $(n^0, e^0)$  and  $(n^1, e^1)$  in  $\mathcal{X}$ , there exist a time  $T \geq 0$  and a solution  $t \mapsto (n(t), e(t), p_n(t), p_e(t))$  of (34) defined from  $[0, T]$  to  $\mathcal{X}$ , such that  $(n(0), e(0)) = (n^0, e^0)$  and  $(n(T), e(T)) = (n^1, e^1)$ .*

*Proof.* From Proposition 6, it is a consequence of the following theorem 14, with  $\bar{\lambda} = -\frac{1}{3} \ln(n^1/n^0)$ ,  $e^0 = \sin \varphi^0$ ,  $e^1 = \sin \varphi^1$ .  $\square$

**Theorem 14** (geodesic convexity in the variables  $(\psi, \varphi, n)$ ). *For any  $\varphi^0$  and  $\varphi^1$  in the interval  $(-\pi/2, \pi/2)$  and any  $\bar{\lambda} \in \mathbb{R}$ , there exists  $\tau_{\text{fin}} \geq 0$  and a solution  $(\psi(\cdot), \varphi(\cdot)) : [0, \tau_{\text{fin}}] \rightarrow \mathcal{C}$  of (36a)-(36b) such that*

$$\varphi(0) = \varphi^0, \quad \varphi(\tau_{\text{fin}}) = \varphi^1, \quad \int_0^{\tau_{\text{fin}}} c(\psi(\tau), \varphi(\tau)) d\tau = \bar{\lambda}. \quad (64)$$

*Proof.* From Lemma 7, it is sufficient to prove the theorem for  $\varphi^1, \varphi^2$  satisfying

$$-\frac{\pi}{2} < \varphi^0 \leq \varphi^1 < \frac{\pi}{2} \quad \text{and} \quad \varphi^0 \leq 0 \quad (65)$$

because the “+” symmetry allows one to interchange  $\varphi^1$  and  $\varphi^0$  while the “#” symmetry changes their sign. We distinguish four cases:

**Case 1:**  $-\frac{\pi}{2} < \varphi^0 < \varphi^1 < 0$ . The solutions such that  $\varphi(0) = \varphi^0$ ,  $\varphi(\tau_{\text{fin}}) = \varphi^1$  must lie entirely in one of the regions  $E$ ,  $F$  or  $F^+$  or in the stable manifolds  $\mathcal{S}^0$  or  $\mathcal{S}^\pi$  that separate them (see Figure 4). In particular, at time  $\tau_{\text{fin}}$ , they satisfy  $U^0(\varphi^1) < \psi(\tau_{\text{fin}}) < U^\pi(\varphi^1)$ ; at time zero, they satisfy the more restrictive  $Z^b(\varphi^0) < \psi(0) < \pi + Z^b(\varphi^0)$  because a solution with initial condition such that  $U^0(\varphi^0) < \psi(0) < Z^b(\varphi^0)$  or  $\pi + Z^b(\varphi^0) < \psi(0) < U^\pi(\varphi^0)$  never crosses  $\{\varphi = \varphi^1\}$  in positive time. Let us parameterize these solutions by  $\psi(\tau_{\text{fin}})$ , the final value of  $\psi$ :

$$\begin{aligned} &\text{For all } \chi \text{ in the open interval } (U^0(\varphi^1), U^\pi(\varphi^1)), \text{ there exists} \\ &\text{a unique solution } \tau \mapsto (\psi^x(\tau), \varphi^x(\tau)) \text{ and a unique time } \tau_{\text{fin}}^x > 0 \quad (66) \\ &\text{such that } \varphi^x(0) = \varphi^0, \quad \psi^x(\tau_{\text{fin}}^x) = \chi, \quad \varphi^x(\tau_{\text{fin}}^x) = \varphi^1, \end{aligned}$$

and  $\psi^x(\tau), \varphi^x(\tau), \tau_{\text{fin}}^x$  are continuous with respect to  $\chi$  and continuously differentiable with respect to  $\tau$ . Indeed, there is a unique solution  $(\widehat{\psi}^x(\cdot), \widehat{\varphi}^x(\cdot))$  to the Cauchy problem (55) with initial condition  $\widehat{\psi}^x(0) = \chi$ ,  $\widehat{\varphi}^x(0) = \varphi^1$ , defined in positive and negative time; it is continuous with respect to  $\chi$  and continuously differentiable with respect to  $\tau$  (it is even smooth if the trajectory does not cross the curves (31)); if the solution is in  $E$  or the stable manifolds,  $\widehat{\varphi}$  is an increasing function of time, if it is in  $F$  or  $F^+$ , it is first increasing and then decreasing, hence, in both cases, since  $\varphi^0 < \varphi^1$ , there is a unique negative time  $-\tau_{\text{fin}}^x < 0$  such that  $\widehat{\varphi}^x(-\tau_{\text{fin}}^x) = \varphi^0$ , and it satisfies  $Z^b(\varphi^0) < \widehat{\psi}^x(-\tau_{\text{fin}}^x) < \pi + Z^b(\varphi^0)$ , hence  $b(\widehat{\varphi}^x(-\tau_{\text{fin}}^x), \widehat{\psi}^x(-\tau_{\text{fin}}^x)) > 0$ ; this implies that the trajectory intersects *transversely* the circle  $\{\varphi = \varphi^1\}$  at time  $-\tau_{\text{fin}}^x$ , hence  $\tau_{\text{fin}}^x$  depends continuously on  $\chi$ . Take

$$(\psi^x(\tau), \varphi^x(\tau)) = (\widehat{\psi}^x(\tau - \tau_{\text{fin}}^x), \widehat{\varphi}^x(\tau - \tau_{\text{fin}}^x)); \quad (67)$$

(66) is then satisfied. This allows to define a continuous map  $\Lambda$  from the open interval  $(U^0(\varphi^1), U^\pi(\varphi^1))$  to  $\mathbb{R}$  by

$$\Lambda(\chi) = \int_0^{\tau_{\text{fin}}^x} c(\psi^x(s), \varphi^x(s)) ds. \quad (68)$$

We now prove that

$$\lim_{\substack{\chi \rightarrow S^0(\varphi^1) \\ \chi > S^\pi(\varphi^1)}} \Lambda(\chi) = +\infty, \quad \lim_{\substack{\chi \rightarrow S^0(\varphi^1) \\ \chi < S^\pi(\varphi^1)}} \Lambda(\chi) = -\infty. \quad (69)$$

Let us give a very elementary proof of these limits (although they are consequences of very classical facts about the behavior of trajectories that join points very close to a stable manifold to points very close to the unstable manifold). Consider again the solutions  $(\widehat{\psi}^x(\cdot), \widehat{\varphi}^x(\cdot))$  to the Cauchy problem (55) with initial condition  $\widehat{\psi}^x(0) = \chi$ ,  $\widehat{\varphi}^x(0) = \varphi^1$ ; they can be defined for  $\chi$  outside the interval  $(U^0(\varphi^1), U^\pi(\varphi^1))$ ; for  $\chi = U^0(\varphi^1)$ , this solution lies on the unstable manifold  $\mathcal{U}^0$ , it defined for all negative time and tends to  $(0, 0)$  as time  $\tau$  tends to  $-\infty$ ; to prove the first limit in

(69), take  $M$  arbitrarily large and  $\Omega$  a neighborhood of  $(0, 0)$  such that  $c(\psi, \varphi) > \frac{1}{2}$  when  $(\psi, \varphi)$  is in  $\Omega$  (recall that  $c(0, 0) = 1$ ); let  $T > 0$  be such that

$$\tau \leq -T \Rightarrow (\widehat{\psi}^{U^0(\varphi^1)}(\tau), \widehat{\varphi}^{U^0(\varphi^1)}(\tau)) \in \Omega;$$

the solution  $(\widehat{\psi}^\chi(\cdot), \widehat{\varphi}^\chi(\cdot))$  converges uniformly to  $(\widehat{\psi}^{U^0(\varphi^1)}(\cdot), \widehat{\varphi}^{U^0(\varphi^1)}(\cdot))$  on the finite time interval  $[-T - 4M, 0]$  as  $\chi$  tends to  $U^0(\varphi^1)$ , and this implies that, for  $\chi$  close enough to  $U^0(\varphi^1)$ ,  $(\widehat{\psi}^\chi(\tau), \widehat{\varphi}^\chi(\tau)) \in \Omega$  for all  $\tau$  in  $[-T - 4M, -T]$ , hence  $\tau_{\text{fin}}^\chi > T + 4M$  and  $\int_{-T}^{-T-4M} c(\widehat{\psi}^\chi(\tau), \widehat{\varphi}^\chi(\tau)) d\tau > M$ ; now, according to (67),  $\int_{-T-4M}^{-T} c(\widehat{\psi}^\chi(\tau), \widehat{\varphi}^\chi(\tau)) d\tau = \int_{\tau_{\text{fin}}^\chi - T - 4M}^{\tau_{\text{fin}}^\chi - T} c(\psi^\chi(\tau), \varphi^\chi(\tau)) d\tau$ , and then, if  $U^0(\varphi^1) < \chi < S^0(\varphi^1)$ , since  $c$  is positive in the region “F”, this implies  $\int_0^{\tau_{\text{fin}}^\chi} c(\psi^\chi(\tau), \varphi^\chi(\tau)) d\tau > \chi < S^0(\varphi^1)$ , since  $c$  is positive in the region “F”, this implies  $\int_0^{\tau_{\text{fin}}^\chi} c(\psi^\chi(\tau), \varphi^\chi(\tau)) d\tau > M$ . This proves the first limit in (69); the second one follows in the same way. Since  $\Lambda$  is continuous, (69) implies that it is onto  $\mathbb{R}$ , i.e. there exists, for all  $\lambda \in \mathbb{R}$ , a solution  $(\psi^\chi(\cdot), \varphi^\chi(\cdot))$  and a time  $\tau_{\text{fin}}^\chi$  such that  $\varphi^\chi(0) = \varphi^0$ ,  $\varphi^\chi(\tau_{\text{fin}}^\chi) = \varphi^1$  and  $\Lambda(\chi) = \bar{\lambda}$ . QED.

**Case 2:**  $-\frac{\pi}{2} < \varphi^0 = \varphi^1 < 0$ . It is similar to the previous case but degenerated in that the only nontrivial trajectories that display the same initial and final values of  $\varphi$  lie in the regions  $F$  or  $F^+$ , and they join points on one side of the curve where  $b$  vanishes ( $\psi = Z^b(\varphi)$  or  $\psi = \pi + Z^b(\varphi)$ ) to points on the other side; formally, (66) still holds but  $\tau_{\text{fin}}^\chi$  is zero for all  $\chi$  between  $Z^b(\varphi^1)$  and  $\pi + Z^b(\varphi^1)$ ; the continuity arguments hold for  $\chi$  outside  $[Z^b(\varphi^1), \pi + Z^b(\varphi^1)]$ , one has

$$\Lambda(\chi) \begin{cases} > 0 & \text{if } U^0(\varphi^1) < \chi < Z^b(\varphi^1), \\ = 0 & \text{if } Z^b(\varphi^1) \leq \chi \leq \pi + Z^b(\varphi^1), \\ < 0 & \text{if } \pi + Z^b(\varphi^1) < \chi < U^\pi(\varphi^1), \end{cases}$$

and the same arguments prove that  $\Lambda$  is onto.

**Case 3:**  $\varphi^0 = \varphi^1 = 0$  is very simple: it suffices to chose  $\tau_{\text{fin}} = |\bar{\lambda}|$  and the solution to be the equilibrium  $(0, 0)$  if  $\bar{\lambda} \geq 0$  or the equilibrium  $(\pi, 0)$  if  $\bar{\lambda} \leq 0$ ; then (64) is satisfied because  $c(0, 0) = 1$ ,  $c(\pi, 0) = -1$ .

**Case 4:**  $-\frac{\pi}{2} < \varphi^0 \leq 0 \leq \varphi^1 < \frac{\pi}{2}$ ,  $\varphi^0 < \varphi^1$ . This is the other “generic” case, with case 1. The solutions such that  $\varphi(0) = \varphi^0$ ,  $\varphi(\tau_{\text{fin}}) = \varphi^1$  must lie in the region “E” (see Figure 4) and satisfy  $S^0(\varphi^0) < \psi(0) < S^\pi(\varphi^0)$ ,  $U^0(\varphi^1) < \psi(\tau_{\text{fin}}) < U^\pi(\varphi^1)$ . It is slightly simpler than case 1: here, we may parameterize these solutions by the initial value of  $\psi$  whereas it was impossible in case 1 because the same initial value could, in that case, yield two different times where the same solution crossed  $\{\varphi = \varphi^1\}$ , yielding two different final values for  $\psi$ .

One could write a simpler proof for this case, but the same proof as in case 1 is also valid. Property (66) still holds although the picture is different and all solutions are in the region  $E$ , joining points below the axis  $\{\varphi = 0\}$  to points above this axis; the following arguments hold too, with only a slight modification: in the proof of the limits (69), if  $\varphi^1 = 0$  (hence  $\varphi^0 < 0$ ), the solution  $(\widehat{\psi}^{U^0(\varphi^1)}(\cdot), \widehat{\varphi}^{U^0(\varphi^1)}(\cdot))$  is the equilibrium point  $(0, 0)$ , hence one may take  $T = 0$  for any neighborhood  $\Omega$ .  $\square$

## 5. COMPARISON BETWEEN THE ENERGY AND MINIMUM-TIME CASES FROM THE CONVEXITY POINT OF VIEW

We recalled in section 3 some results from [2] (and previous work by the same authors); in particular, Theorem 3 states that the elliptic domain is *not* geodesically

convex for the energy minimization problem, i.e. some pair of points in  $\mathcal{E}$  cannot be joined by a geodesic. Since geodesics are straight lines in suitable coordinates (polar coordinates  $(n^{5/6}, \sqrt{5/2}\varphi)$ ), the simplest way to see this non convexity is to determine the shape on the elliptic domain in these coordinates where geodesic convexity reduces to usual (affine) convexity and to see that it is *not* convex.

Here we try to understand why convexity holds in the minimum time case and not the energy case. Using the coordinates from Theorem 3 for the time-minimizing problem does not seem to shed any light. On the contrary, we shall explain why the proof of convexity that we made in the time-minimum case fails when applied to the energy minimizing case.

The Hamiltonian is given by (17), and can be written as follows, when  $p_\omega = 0$

$$H = n^{-5/3} [2(3n p_n)^2 + 5p_\varphi^2] \quad (70)$$

in the coordinates  $(n, \varphi, p_n, p_\varphi)$  that result from the symplectic change of coordinates  $e = \sin \varphi$ ,  $p_\varphi = \sqrt{1 - e^2} p_e$ . The Hamiltonian equations can be written

$$\begin{aligned} \dot{n} &= 12 n^{-2/3} (3n p_n), & \frac{d}{dt}(3n p_n) &= 5n^{-5/3} [2(3n p_n)^2 + 5p_\varphi^2], \\ \dot{\varphi} &= 10 n^{-5/3} p_\varphi, & \dot{p}_\varphi &= 0. \end{aligned}$$

With the same polar coordinates as in (21), namely  $\rho \cos \psi = 3n p_n$ ,  $\rho \sin \psi = -p_\varphi$ , and the change of time  $dt = 5n^{-5/3} d\tau$ , one gets

$$d\psi/d\tau = -\sin \psi (2 + 3 \sin^2 \psi), \quad d\varphi/d\tau = 2 \sin \psi. \quad (71)$$

It is easy to describe the solutions of these on the cylinder  $\mathcal{C}$  (see (30)). There are

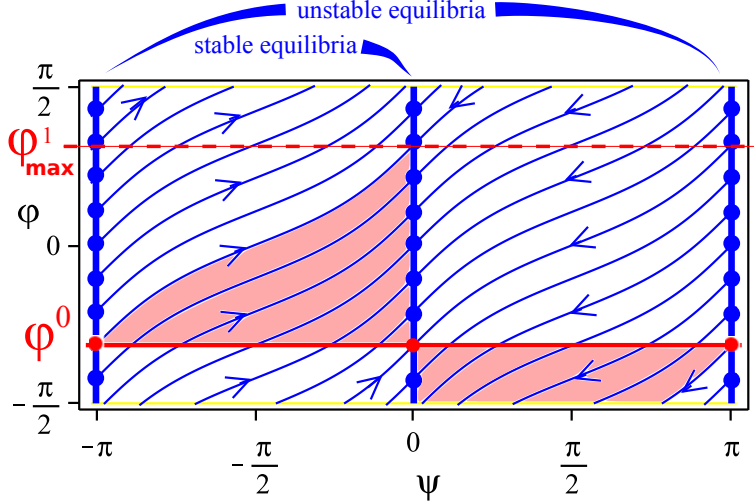


FIGURE 5. The phase portrait, for energy minimization, in the same coordinates as Figure 4. There are two lines of non isolated equilibria. The darker zone is all the points that can be reached in positive time from the line  $\{\varphi = \varphi^0\}$ , with  $\varphi^0$  rather close to  $-\frac{\pi}{2}$ . The highest possible final value is  $\varphi$  is  $\varphi_{\max}^1 = \varphi^0 + \sqrt{2/5}\pi$ .

two lines of equilibria at  $\psi = 0$  and  $\psi = \pi$  and

$$\varphi + \sqrt{\frac{2}{5}} \arctan \left( \sqrt{\frac{5}{2}} \tan \psi \right) \quad (72)$$

is a first integral (it is smooth at  $\psi = \frac{\pi}{2}$ ). These solutions are drawn on Figure 5. It is clear that, on a solution,  $\varphi$  can vary at most by  $\sqrt{2/5}\pi$ , and this implies that, if  $|\varphi^0| > (\sqrt{2/5} - \frac{1}{2})\pi$ , there are some values of  $\varphi$  that cannot be reached by any solution starting from the line  $\{\varphi = \varphi^0\}$ .

#### REFERENCES

- [1] A. Bombrun and J.-B. Pomet. The averaged control system of fast oscillating control systems. *SIAM J. Control Optim.*, 51(3):2280–2305, 2013.
- [2] B. Bonnard and J.-B. Caillau. Geodesic flow of the averaged controlled Kepler equation. *Forum Mathematicum*, 21(5):797–814, Sept. 2009.
- [3] B. Bonnard, J.-B. Caillau, and R. Dujol. Energy minimization of single input orbit transfer by averaging and continuation. *Bull. Sci. Math.*, 130(8):707–719, 2006.
- [4] B. Bonnard, L. Faubourg, and E. Trélat. *Mécanique céleste et contrôle des véhicules spatiaux*, volume 51 of *Mathématiques & Applications*. Springer-Verlag, Berlin, 2006.
- [5] T. N. Edelbaum. Optimum low-thrust rendezvous and station keeping. *AIAA J.*, 2:1196–1201, 1964.
- [6] T. N. Edelbaum. Optimum power-limited orbit transfer in strong gravity fields. *AIAA J.*, 3:921–925, 1965.
- [7] S. Geffroy. *Généralisation des techniques de moyennation en contrôle optimal - Application aux problèmes de rendez-vous orbitaux en poussée faible*. Thèse de doctorat, Institut National Polytechnique de Toulouse, Toulouse, France, Oct. 1997.
- [8] S. Geffroy and R. Epenoy. Optimal low-thrust transfers with constraints-generalization of averaging technics. *Acta Astronautica*, 41(3):133–149, 1997.

INSTITUT DE MATHÉMATIQUES DE BOURGOGNE, UNIVERSITÉ DE BOURGOGNE, 9 AVENUE ALAIN SAVARY, 21078 DIJON, FRANCE. ON LEAVE TO INRIA SOPHIA ANTIPOLIS MÉDITERRANÉE, McTAO, 2004 ROUTE DES LUCIOLES, 06902 SOPHIA ANTIPOLIS CEDEX

*E-mail address:* `bernard.bonnard@u-bourgogne.fr`

INRIA SOPHIA ANTIPOLIS MÉDITERRANÉE, McTAO, 06902 SOPHIA ANTIPOLIS, FRANCE

*E-mail address:* `helen-clare.henninger@inria.fr`

DEPARTMENT OF MATHEMATICS, INSTITUTE OF CHEMICAL TECHNOLOGY, TECHNICKÁ 5, 166 28 PRAGUE 6, CZECH REPUBLIC

*E-mail address:* `Jana.Nemcova@vscht.cz`

INRIA SOPHIA ANTIPOLIS MÉDITERRANÉE, McTAO, 06902 SOPHIA ANTIPOLIS, FRANCE

*E-mail address:* `jean-baptiste.pomet@inria.fr`